LA--10369-MS

DE85 011892

Iron and Manganese in Oxide Minerals and in Glasses: Preliminary Consideration of Eh Buffering Potential at Yucca Mountain, Nevada

F. A. Caporuscio*
D. T. Vaniman

*Consultant at Los Alamos. Department of Geology, University of Colorado, Boulder, CO 80309.

Los Alamos National Laboratory
Los Alamos, New Mexico 87545

IRON AND MANGANESE IN OXIDE MINERALS AND IN GLASSES: PRELIMINARY CONSIDERATION OF Eh BUFFERING POTENTIAL AT YUCCA MOUNTAIN, NEVADA

by

F. A. Caporuscio and D. T. Vaniman

ABSTRACT

The tuffs of Yucca Mountain at the Nevada Test Site are currently under investigation as a possible deep burial site for high-level radioactive waste disposal. One of the main concerns is the effect of oxidizing groundwater on the transport of radionuclides. Rock components that may affect the oxygen content of groundwater include Fe-Ti oxides, Mn oxides, and glasses that contain ferrous iron.

Some phenocryst Fe-Ti oxides at Yucca Mountain are in reduced states, whereas groundmass Fe-Ti oxides have been oxidized to hematite, rutile, and pseudobrookite (Fe^{3+}-bearing phases) exclusively. Estimates of Fe^{2+}-bearing oxides indicate that less than 0.33 vol% phenocrysts is available to act as solid buffering agents of Eh. Of this percentage, significant amounts of Fe-Ti oxides are isolated from effective interaction with groundwater because they occur in densely welded, devitrified tuffs that have low interstitial permeability.

Manganese oxides occur primarily along fractures in the ash-flow tuffs. Because the Mn oxides are concentrated along the same pathways (fractures) where transport has occurred in the past, these small volume percentages could act as buffers. However, the oxidation states of actual Mn-oxide phases are high (Mn^{4+}), and these minerals have virtually no potential for reducing groundwater Eh. Manganese oxides may even act as oxidizing agents. However, regardless of their poor capabilities as reducing agents, the Mn oxides could be important as sorbents of heavy metals at Yucca Mountain. The lack of accessible, pristine Fe-Ti oxides and the generally high oxidation states of Mn oxides seem to rule out these oxides as Eh buffers of the Yucca Mountain groundwater system. Reduction of ferrous iron within glassy tuffs may have some effect on Eh, but further study is needed. At present it is prudent to assume that minerals and glasses have little or no capacity for reducing oxygen-rich groundwater at Yucca Mountain.

I. INTRODUCTION

The southwestern portion of the Nevada Test Site (NTS) in south-central Nevada is being studied to determine the suitability of the area for an underground high-level waste repository. This report is one of the continuing studies, sponsored by the Nevada Nuclear Waste Storage Investigations (NNWSI), concerned with the tuff units of Yucca Mountain and the suitability of these units for waste isolation. The NNWSI Project is managed by the Nevada Operations Office of the Department of Energy. The exploration drill holes mentioned in this report (USW G-1, G-2, G-3, GU-3, G-4, USW H-6, UE-25p#1, UE-25a#1, and UE-25b#1) are on or near Yucca Mountain near the southwest border of the NTS (Fig. 1). The Yucca Mountain block is composed of a thick sequence of ash-flow tuffs, lavas, and bedded tuffs that have been derived primarily from the Timber Mountain-Oasis Valley caldera complex (Byers et al. 1976; Christiansen et al. 1977). The thickness of tuffs at Yucca Mountain exceeds 6000 ft (1830 m) and may extend to 10 000 ft (3050 m). The tuffs range in age from 15 to 12 Myr.

Oxide minerals (also referred to as "opaques" because of their optical properties) can remove oxygen from groundwater if the oxide minerals contain oxidizable Fe^{2+} or Mn^{2+}. The primary objective of this report is to estimate the distribution and volume percentages of Fe^{2+}-bearing oxide minerals in the Yucca Mountain block. If present in sufficient abundance, these minerals (magnetite and ilmenite) could buffer groundwater oxygen content at Yucca Mountain. Several waste radionuclides have lower solubilities under reducing conditions than under oxidizing conditions, e.g., Tc, U, Np, Pu (Ogard and Kerrisk 1984). This work is primarily to determine whether enough FeO is accessible in the Yucca Mountain block to efficiently buffer the water Eh and thereby limit the solubilities of such waste elements. The Fe-Ti oxides occur as both phenocrysts and groundmass grains. This report discusses which Fe-Ti oxides are in a pristine (reduced) form and presents oxidation-exsolution data for these oxides (Appendix A). Zones of high- and low- Fe-Ti-oxide oxidation are also discussed in this paper, with particular emphasis on low-oxidation zones.

A secondary objective of this report is to identify the types and abundances of Mn oxides that are concentrated in tuff fractures (open and closed) at Yucca Mountain. These variable-composition oxides have limited potential as groundwater buffers but may provide additional sorption within

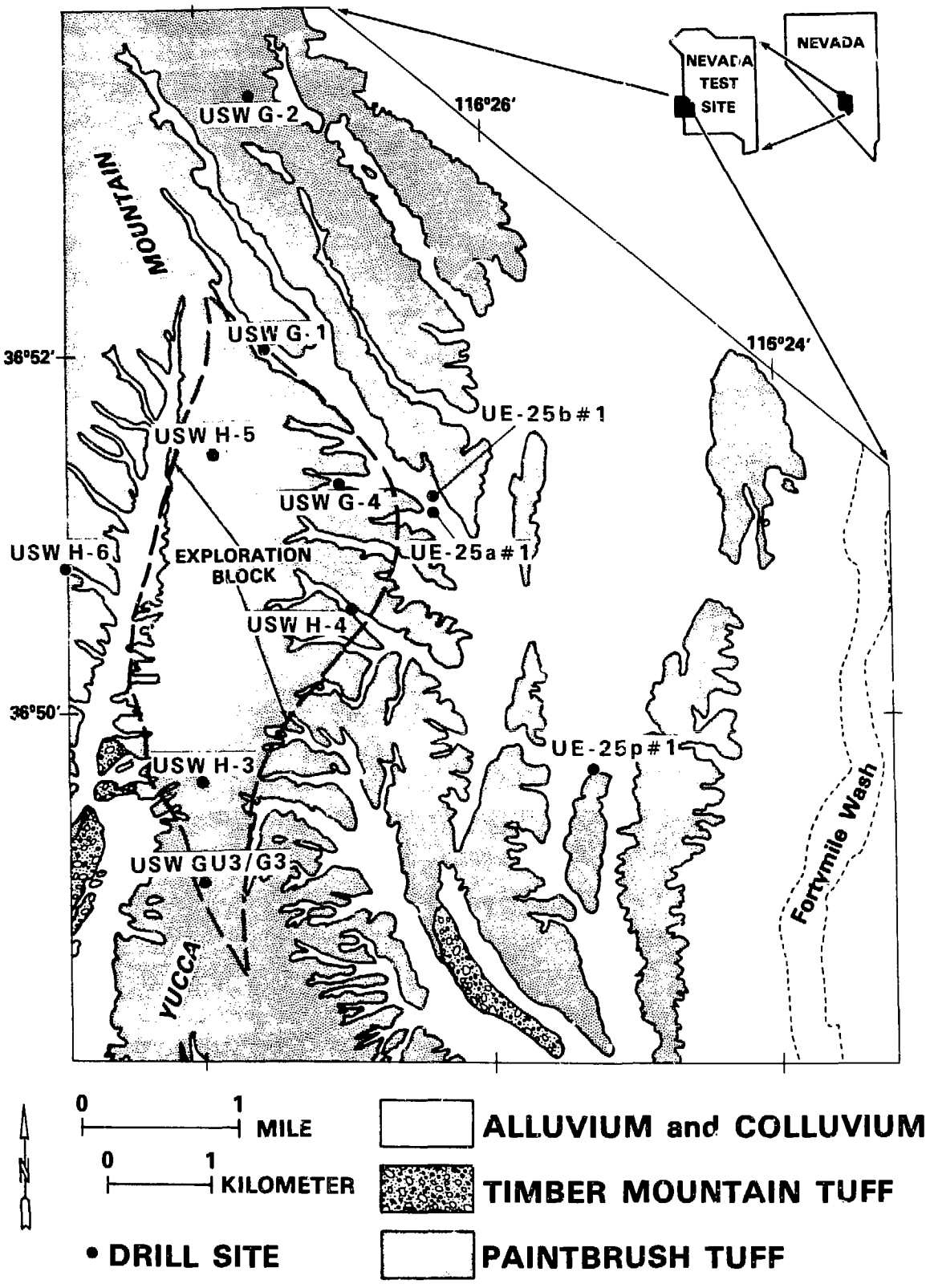

Fig. 1. Index map of Yucca Mountain, including pertinent drill holes.

fractures. The source of Mn for Mn fracture fill is discussed in Sec. V of this paper.

II. METHODS

Both cubic and rhombohedral Fe-Ti oxides are ubiquitous in the tuffs and rarer lavas of Yucca Mountain. These oxides are useful because they reflect the extent of groundwater-tuff interaction, the permeability of the enclosing rocks, and the maximum oxidation state of the rock (see Bish et al. 1981; Caporuscio et al. 1982). Haggerty (1976a) developed an empirical method, using reflected-light microscopy, to evaluate the oxidation state of Fe-Ti-oxide phenocrysts in basalts. His method of evaluating and characterizing oxidation exsolution textures in Fe-Ti oxides (Table I) has been adapted to our investigation of high-silica rocks.

The Fe-Ti oxides are observed as microphenocrysts and as alteration products in the ash flows and lavas. Morphologies indicate that both cubic [magnetite-ülvospinel solid-solution series ($Mt\text{-}\ddot{U}sp_{ss}$)] and rhombohedral [ilmenite-hematite solid-solution series ($Ilm\text{-}Hem_{ss}$)] phases exist. Subsequent oxidation of the Fe-Ti oxides after eruption produced a series of oxidation-exsolution phases within the original grains. Haggerty's (1976a) classification for the cubic (C_1 to C_7) and rhombohedral (R_1 to R_7) phases is retained for this study, where subscript 1 denotes the unoxidized phase and subscript 7 denotes complete oxidation of the phase. In all cases, the oxidation state of the $Ilm\text{-}Hem_{ss}$ closely parallels that of the $Mt\text{-}\ddot{U}sp_{ss}$. Therefore, all oxides reported are given a C_x notation for consistency. The oxidation state of the Fe-Ti oxides depends on the highest ambient fO_2 (oxygen fugacity), which may often be correlated with the interstitial permeability and degree of welding of the tuffs. It is important to differentiate transmissibility, which may be high in densely welded fractured tuffs and low in nonwelded tuffs, and the interstitial permeability that is generally low in densely welded tuff but high in nonwelded tuff (Winograd and Thordarson 1975). In nonwelded tuffs (high interstitial permeability), the Fe-Ti oxides are generally oxidized (C_5-C_7). Densely welded tuffs (low interstitial permeability) generally record low oxidation states (C_1-C_3). Because of oxidation-exsolution kinetics, the retrograde process is extremely sluggish; therefore, the oxidation state recorded is the highest oxygen fugacity obtained and does not always indicate the present oxygen fugacity in the tuffs.

TABLE I. EXSOLUTION OXIDATION OF Fe-Ti OXIDE CUBIC AND RHOMBOHEDRAL PHASES[a]

Cubic		Rhombohedral	
C_1	magnetite	R_1	ilmenite
C_2	magnetite (+ ilmenite)	R_2	ilmenite + rutile
C_3	ilmenite + magnetite	R_3	rutile + ilmenite
C_4	mottled ilmenite + magnetite + rutile + hematite + pleonaste (meta-ilmenite)	R_4	rutile + titanohematite + ferrian rutile + ferrian ilmenite
C_5	rutile + titanohematite	R_5	rutile + titanohematite
C_6	rutile + titanohematite (+ pseudobrookite)	R_6	rutile + titanohematite + (pseudobrookite)
C_7	pseudobrookite + (titanohematite + rutile)	R_7	pseudobrookite + (rutile + titanohematite)

[a] Haggerty, 1976a.

Major exceptions to the scheme described above occur in rocks containing sulfides, carbonates, or vapor-phase alteration. For example, in the densely welded portion of the Topopah Spring Member where vapor-phase minerals are present, the oxidation state varies greatly. This occurs because vapor-phase fluids have high water content and therefore have a high oxygen fugacity. Oxidation state is controlled by vapor-phase fluids that may intersect a particular grain. In many samples, oxide grains in proximity can have radically different oxidation states. In rocks containing sulfides or carbonates, oxygen fugacity is decreased and the oxidation of Fe-Ti-oxide minerals is retarded. Either of these fluids (S- or CO_2-bearing) would have a much lower fO_2 than one bearing H_2O only. Therefore, these fluids may oxidize the Fe-Ti oxides but to a lesser extent. Specific examples are given in Sec. III of this report.

The content of ferrous iron in bulk-rock samples is discussed in Sec. VII. Determinations of ferrous iron were made by the method of Bower (1984), based on spectrophotometric determination. The precision of this method is better than 0.2 wt% FeO.

III. OXIDES WITHIN THE YUCCA MOUNTAIN BLOCK

During this study, over 430 polished thin sections of tuff and lava from nine drill holes were examined by reflected-light microscopy for Fe-Ti-oxide

phenocrysts. Between 10 and 20 phenocrysts were characterized for oxidation exsolution in each thin section. The average oxidation state is the sum of the individual oxidation-state values divided by the number of oxides examined in a thin section. These average oxidation states are summarized in Fig. 2 for all nine drill holes. More detailed information on the oxidation state of Fe-Ti oxides can be obtained from the appropriate drill-hole characterization report (Bish et al. 1981; Carroll et al. 1981; Caporuscio et al. 1982; Vaniman et al. 1984) and from Appendix A. Most consistent trends, however, are apparent in Fig. 2.

Regions in the tuffs and lavas of Yucca Mountain that have an average oxidation state of C_4 or less are depicted by a stippled pattern in Fig. 2. The reason for highlighting these regions is the presence of Fe^{2+} in the cubic ($Mt\text{-}Usp_{ss}$) and, rhombohedral ($Ilm\text{-}Hem_{ss}$) opaques. The regions thus depicted still contain magnetite ($Fe^{2+}O{:}Fe_2^{3+}O_3$) and ilmenite ($Fe^{2+}TiO_3$) in varying quantities. Significant quantities of iron in the reduced state could buffer water in the Eh range of -0.2 to 0.0 V for pH in the range from 6 to 8 (Garrels and Christ 1965).

Figure 2 lists numerous zones where the average oxidation state is less than or equal to four. These zones occur in both the saturated and unsaturated zones of Yucca Mountain. Unoxidized opaques are not expected in the saturated zones because of water interaction; therefore, these low-oxidation zones require explanation. We noted earlier that S- and CO_2-bearing fluids suppress the oxidation state of Fe-Ti oxides (Caporuscio et al. 1982). Clear examples are seen in drill cores USW G-2, UE-25a#1/b#1, and USW G-3/GU-3 (Fig. 2). In those zones with sulfides, the oxides are relatively unoxidized compared with surrounding tuff units. Similarly, carbonate-rich zones in USW G-1 (~5200 - 6000 ft) and UE-25p#1 (~3700 - 3800 ft) exhibit suppressed oxidation states (C_4 or less). Another environment in the saturated zone where Fe-Ti-oxide phenocrysts are commonly C_4 or less is in dacitic to rhyolitic lavas. These lavas and their associated slightly oxidized opaques are readily apparent in USW G-1 (~3350 - 3900 ft) and in USW G-2 (5000 to 5200 ft and 5650 to 6000 ft). Opaques in the lavas are only slightly oxidized due to the low permeability of the flows. The remaining low-oxidation region in the saturated zone (~1900 to 2100 ft in USW G-1) is caused by very low interstitial permeability in the densely welded zone of the Prow Pass member of the Crater Flat Tuff.

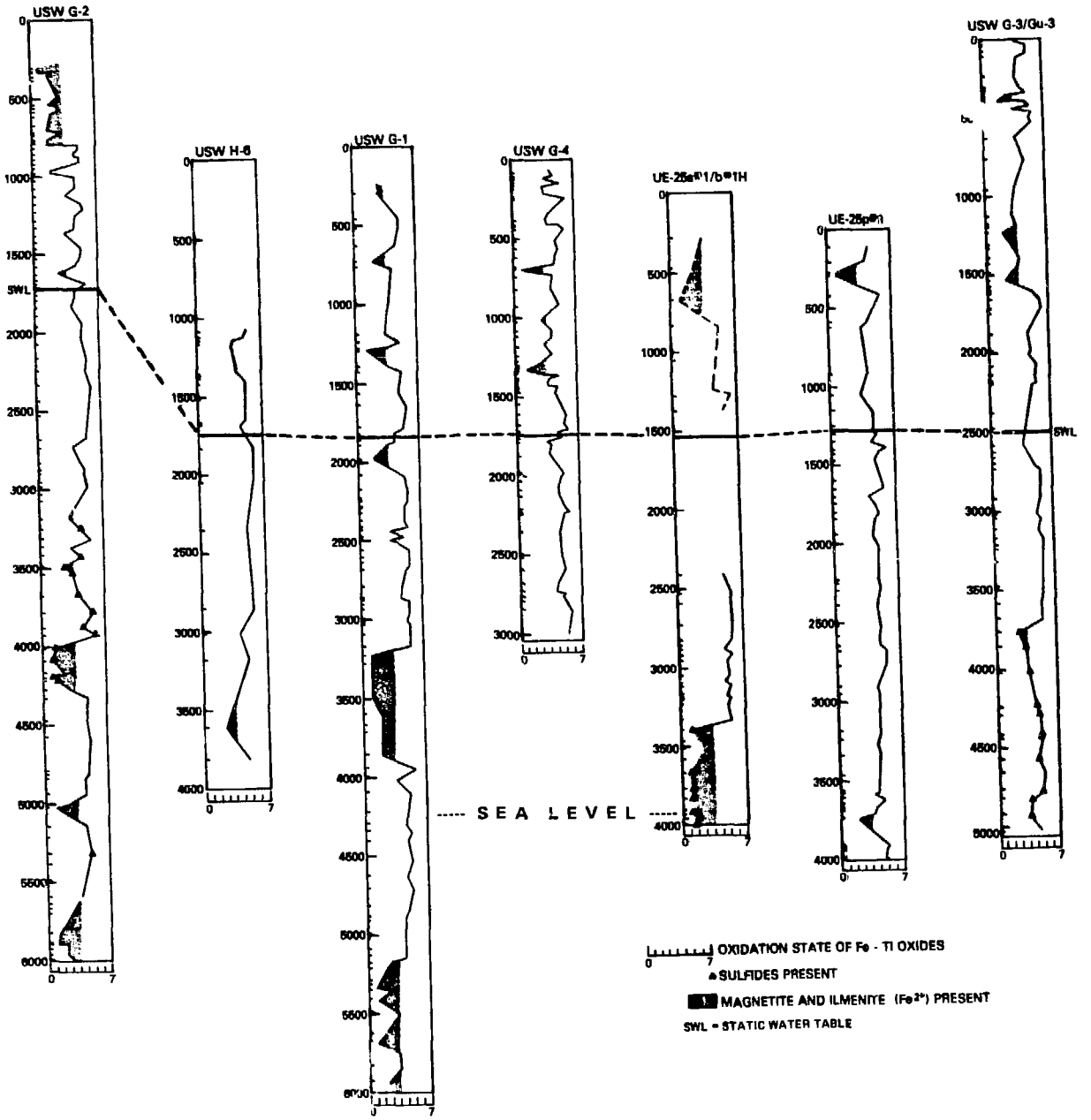

Fig. 2. Oxidation states of Fe-Ti oxides at Yucca Mountain. Note that oxidation state increases from left to right and that shaded regions are less than or equal to C_4. Depths from surface (in feet) are listed along each column; columns are justified to datum for lateral comparison.

All other regions where the Fe-Ti-oxide phenocrysts still retain some primary magnetite or ilmenite are in the unsaturated zone at Yucca Mountain. Specifically, all nonoxidized zones are associated with either the upper and lower vitrophyres of the Topopah Spring member (for example, 400 ft and 1300-1400 ft of USW G-3) or with densely welded zones (~700 ft in G-4, uppermost G-2, ~750 ft in G-1, and 500-600 ft in UE-25a#1). The only exception is at approximately 1500 ft in drill core USW G-3/GU-3. In this instance, the nonoxidized opaques occur in the nonwelded, unaltered vitric tuff of Calico Hills above the static water level. All other non- to slightly oxidized opaques in the unsaturated zone are in densely welded tuff of low interstitial permeability.

IV. ESTIMATION OF Fe^{2+} REMAINING IN Fe-Ti OXIDES AT YUCCA MOUNTAIN

Using the Fe-Ti-oxide mineral oxidation-exsolution studies of the drill cores presented in Fig. 2, we attempted to estimate the amount of magnetite and ilmenite remaining at Yucca Mountain. This estimate was based on three assumptions. First, we assumed that the modal abundances of oxides in the USW G-1 core were reasonable estimates of the volume of oxides in the Yucca Mountain block as a whole. That is, we assumed that the relative volume of oxides in an ash-flow tuff has little lateral variability. We further assumed that USW G-1 is representative of overall mineralogy, and its proximity to the exploration block will certainly produce data pertinent to that region. Second, two researchers have produced different modal abundances for opaques in USW G-1 and these values were used as upper and lower limits. Byers et al. (1976) reported 1.64 modal% opaques (upper limit), whereas Caporuscio et al. (1982) reported 0.90 modal% opaques (lower limit) in USW G-1. And third, we assumed that we could make a reasonable estimate of the amount of ilmenite and magnetite in oxidized opaques.

As can be seen in Table I, there is no ilmenite or magnetite in phenocrysts denoted by R_5 to R_7 or C_5 to C_7. In the case of C_4, the grain contains about 40% magnetite plus ilmenite, whereas R_4 has approximately 25% ilmenite. The remainder of the C series (C_1 to C_3) describes a progressive transition from Ti-rich magnetite (Fe_2^{2+} Ti) to Ti-poor magnetite (Fe^{2+} Fe_2^{3+}), along with the formation of exsolved ilmenite (Fe^{2+} Ti) in supplementary proportions. This oxidation series can be described as follows: C_1 = 100% Mt, C_2 = 75% Mt, 25% Ilm, C_3 = 50% Mt, 50% Ilm. For the rhombohedral series, any oxidation

results in a loss of Fe^{2+}-bearing ilmenite to produce rutile and titanohematite, or pseudobrookite. The examples are as follows: R_1 = 100% Ilm, R_2 = 75% Ilm, R_3 = 50% Ilm, and R_4 = 25% Ilm. These percentages are used to generate columns 3 and 4 in Table II.

To calculate the volume percentage of Fe^{2+}-bearing opaques (magnetite and ilmenite) at Yucca Mountain, we combined the assumptions stated previously about modal percentages and ratios of ilmenite and magnetite (that is, R_3 = 50% ilmenite) to set both lower and upper limits. In Table II, column 1 is the percentage of samples with an average oxidation state of C_4 (or R_4) or less. These samples range from a high of 40% in USW G-2 to a low of 15% in UE-25p#1, with an average of 29% for the Yucca Mountain block. Column 2 indicates the maximum possible volume percentage of oxides if all opaques are magnetite, if those phenocrysts are unoxidized, and if the volume percentage of oxides used is 0.90 modal% [value from Caporuscio et al. (1982) for USW G-1]. The only change in column 3 is that C_4 oxides are now weighted at 40% Fe^{2+}-bearing phases. Therefore, all samples that have an average oxidation state of C_4 contain only 40% magnetite plus ilmenite in their phenocrysts. Column 3 indicates that if all Fe-Ti oxides in the Yucca Mountain block were originally 0.90 vol% magnetite, only 0.23 vol% remains because of subsequent oxidation. Similarly, column 4 reports calculations assuming that all opaques were originally ilmenite phenocrysts. By using the percentages in column 2 and factoring in the percentage of ilmenite lost to oxidation, we obtained the results in column 4. The oxidation factor for ilmenite was discussed previously (that is, R_1 = 100% ilmemite, R_2 = 75% ilmenite, 25% rutile, etc.). This correction factor takes into account the fact that an R_2 phenocryst contains only 75% by volume of an Fe^{2+}-bearing phase, with further losses for R_3 and R_4. The average value of remaining ilmenite (assuming ilmenite phenocrysts only and 0.9 modal% opaques) in Yucca Mountain is 0.14 vol%.

We calculated columns 3 and 4 for simplicity; however, it would be wrong to believe that the opaque phenocrysts in the tuffs and lavas of Yucca Mountain were originally either magnetite or ilmenite only. Based on petrographic observations of Yucca Mountain samples, phase equilibria studies (Haggerty 1976b), and studies of other suites of rhyolitic rocks (Lipman 1971; Hildreth 1979), we concluded that magnetite and ilmenite phenocrysts originally occurred in approximately equal proportions. This has been taken into account in column 5. The values listed are the averages of numbers for

TABLE II. VALUES TO CALCULATE REMAINING Fe^{2+}-BEARING OXIDE MINERALS AT YUCCA MOUNTAIN

	1[a]	2[b]	3[c]	4[d]	5[e]	6[f]
USW G-1	35%	0.32%	0.27%	0.18%	0.225%	0.41%
USW G-2	40	0.36	0.31	0.22	0.265	0.48
USW G-3	27	0.25	0.21	0.09	0.15	0.27
USW G-4	33	0.30	0.26	0.11	0.185	0.337
USW H-6	21	0.19	0.16	0.05	0.105	0.19
UE-25b#1	30	0.30	0.26	0.26	0.26	0.47
UE-25p#1	15	0.14	0.12	0.06	0.09	0.16
Average	29%	0.27%	0.23%	0.14%	0.183%	0.331%

[a] Percentage of samples with average oxidation state of C_4 or less.

[b] Maximum volume percentage of unoxidized magnetite (0.9 modal% opaques).

[c] Calculated volume percentage if magnetite only (0.9 modal% opaques).

[d] Calculated volume percentage if ilmenite only (0.9 modal% opaques).

[e] Calculated volume percentage (lower limit), assuming magnetite and ilmenite phenocrysts were originally of equal proportion at time of eruption (0.9 modal% opaques).

[f] Calculated volume percentage (upper limit), assuming magnetite and ilmenite phenocrysts were originally of equal proportion at time of eruption (1.64 modal% opaques).

each drill core from columns 3 and 4. The volume percentages listed in column 5 are the most reasonable estimates for the remaining available Fe^{2+}-bearing phases, ilmenite and magnetite [assuming a lower limit of 0.9 modal% opaques as calculated by Caporuscio et al. (1982)]. The average value listed in column 5 (0.18 vol%) is the lower estimate of available ilmenite and magnetite of the Yucca Mountain block. Column 6 values were calculated using the 1.64 modal% of opaques as determined by Byers et al. (1976) for the USW G-1 core samples. For column 6, the average value (0.33 modal%) is a reasonable upper estimate of available Fe^{2+}-bearing phases for potential buffers.

By analyzing Fe-Ti-oxide phenocryst oxidation and by using the above calculations, we have estimated volume percentages of magnetite and ilmenite available at Yucca Mountain to act as solid buffers. However, these estimates do not represent fully useful Fe^{2+} unless all oxide phenocrysts were available to the groundwater for interaction. Obviously that assumption is not true, and therefore the amount of Fe^{2+}-bearing oxide phases truly available to react

with groundwater as a buffer at Yucca Mountain must be less than the higher estimate of 0.33 modal%. Because most oxides still available for oxidation are above the static water level or are isolated from water in densely welded tuffs and lavas, possibly less than half of the oxides (0.16%) are available as solid buffers. Therefore, it is very unlikely that oxide phenocrysts can still buffer groundwater Eh. Moreover, the more readily available groundmass oxide minerals are already oxidized and therefore are ineffective in controlling Eh. In 430 samples observed so far, we have not yet identified any groundmass oxides as magnetite or ilmenite. The common oxides observed in the groundmass are hematite, goethite and rutile, none of which contains significant Fe^{2+}. Originally, these groundmass oxides were probably magnetite and ilmenite that have been subsequently oxidized. Their rapid oxidation is due to large surface area per volume area (that is, extremely small size) and the ability of water to interact with these small grains. In addition, many of these groundmass oxides are located along grain boundaries where water can interact with the oxides more efficiently. Finally, some groundmass oxides are produced during vapor-phase alteration under high fO_2 conditions. In conclusion, the only Fe-Ti oxides capable of acting as a solid buffer at Yucca Mountain are phenocrysts that make up less than 0.33 modal% of the rock mass and are largely removed from interaction with groundwater.

V. Mn OXIDES: THEIR OCCURRENCE AND ABUNDANCE

The Mn oxides are a diverse series of minerals in which Mn can take on complex oxidation states. Potter and Rossman (1979a) have identified more than 20 valid species of tetravalent and trivalent manganese oxides. These oxides can have varying amounts of water in their structure and have Mn ionic charges of 2+, 3+, 4+, 6+, and 7+ in many combinations. However, Potter and Rossman (1979a) show that most of the Mn-bearing minerals that occur as dendrites in rock fractures contain Mn^{4+} as the dominant oxidation state. In a study of manganese dendrites, Potter and Rossman (1979b) identified most fracture-lining dendrites as todorokite, romanèchite, or a hollandite-group manganese oxide (for example, cryptomelane). They also identified most underground manganese dendrites as todorokite. Potter and Rossman (1979b) found no dendrites with pyrolusite mineralogy and suggested that the term "pyrolusite dendrite" be discontinued.

The Mn-oxide minerals identified at Yucca Mountain are among those that Potter and Rossman (1979b) specify as being typical of manganese dendrites. Todorokite [$(Mn, Ca, Mg)^{2+}\ Mn_3^{4+}O_7 \cdot H_2O$] has been identified in the Tram Member in drill core UE-25b#1H (Caporuscio et al. 1982), and cryptomelane [$KMn_8^{4+,3+}O_{16}$] has been identified in the Tram Member of drill core USW G-3 (Vaniman et al. 1984) and in recent studies of drill core USW G-4 (Fig. 3). Within the Topopah Spring Member of USW GU-3, we used x-ray diffraction studies to identify a Mn-oxide structure that is either lithiophorite [$(Al, Li)Mn^{4+}O_2(OH)_2$] or todorokite. Further work will be done to characterize and interpret the Mn-oxide occurrences at Yucca Mountain, but the analyses available and the studies by Potter and Rossman (1979a, 1979b) of similar Mn-oxide dendrites strongly suggest that Mn^{2+} is a minor component or absent in these oxides. Moreover, manganese oxides with Mn^{2+} would buffer water Eh in a higher range than would iron. Depending on the actual minerals present, Eh could be controlled in the 0.2- to 0.5-V range for pH in the range from 6 to 8 (Garrels and Christ, 1965). For this reason, water buffered by Mn^{2+} would not be as effective in limiting the solubility of waste elements such as uranium as would water buffered by iron. This factor, plus the relative unavailability of Mn^{2+} in either primary or secondary minerals along the flow path, rules out any effective reduction of groundwater Eh by Mn^{2+} at Yucca Mountain.

Of related interest, Zielinski (1983) and Zielinski et al. (1980) have cited hydrated Mn oxides as very strong sorbers of radionuclides and have proposed that Mn oxides in fractures may be a barrier to radionuclide migration. Concentrations of trace elements such as As, Y, and Ce have been found in Mn oxides of the Topopah Spring Member (Vaniman et al. 1984), indicating that these oxides have accumulated petrologically incompatible elements.

Zielinski (1983) performed whole-rock analyses of all major ash flows and lavas at Yucca Mountain. Values for bulk-rock MnO range from <0.02 wt% in the tuff of Calico Hills to 0.32 wt% in the Tram Member, with an average value of 0.06 wt%. Three likely sources of Mn could supply the necessary amount to produce Mn-oxide fracture fill: (1) Mn-bearing desert varnish that partially goes into solution with rain water and is reprecipitated in fractures; (2) Mn-bearing mineral phases, such as Fe-Ti oxides and clinopyroxenes (Caporuscio et al. 1982) that contain up to 1 wt% MnO; and (3) MnO in the original glass of the ash-flow tuffs. More work remains in comparing the Mn content of fresh

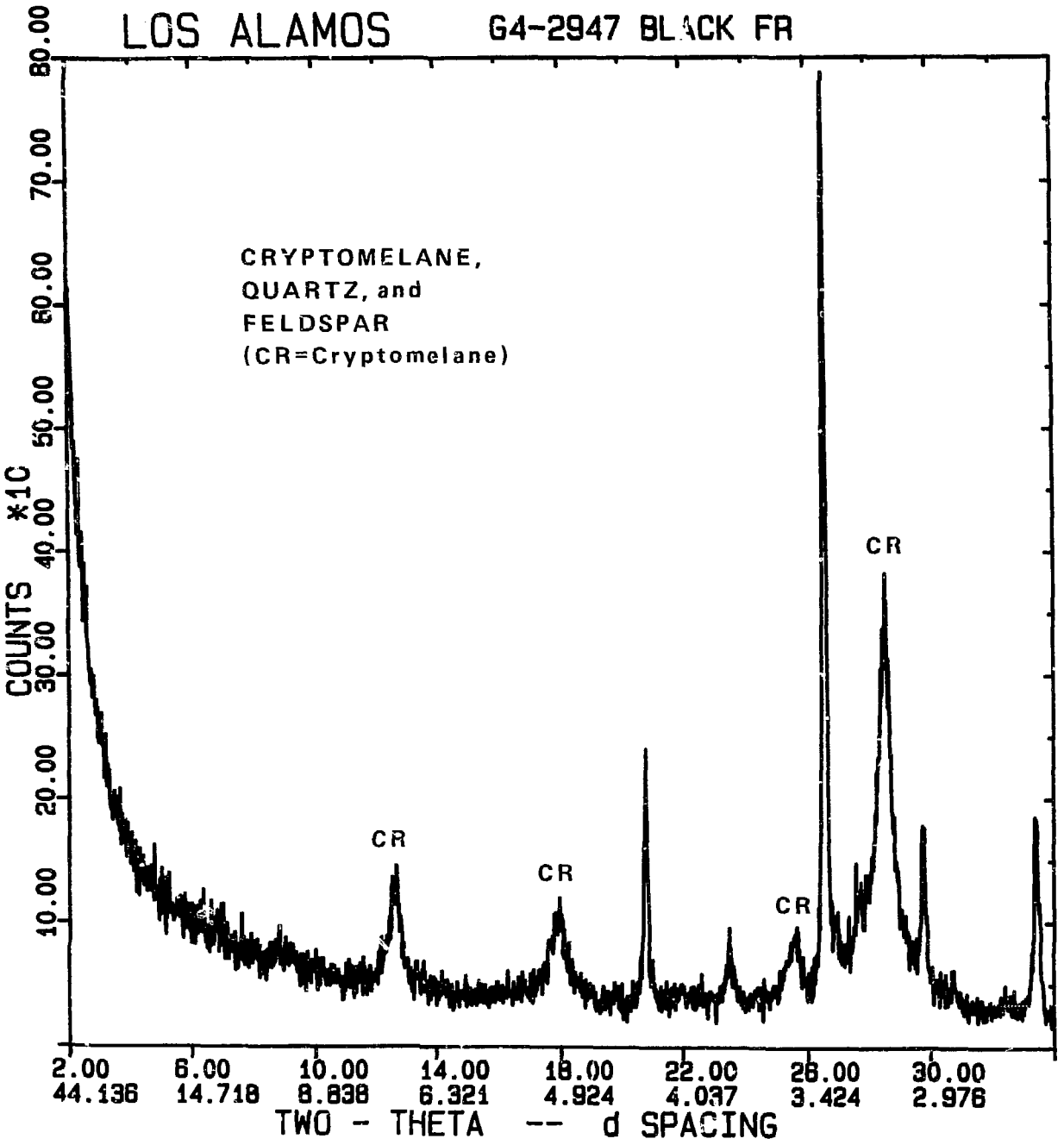

Fig. 3. Representative x-ray diffraction pattern of cryptomelane in USW G-4.

ash flow tuffs with altered ash-flow tuffs (and their mineral compositions) before the source of Mn-oxide fracture fill can be identified with certainty. However, evaluating the potential significance of Mn oxides as sorbents at Yucca Mountain is possible based on Zielinski's work. Zielinski (1983) analyzed small (3-g) samples of bulk tuff for leachable Mn, representing the Mn from sorptive Mn oxides. In samples from the devitrified Topopah Spring Member in USW G-1, these analyses indicate 0.016 wt% Mn oxides in the bulk rock. If a repository area of 7 km^2 in the Topopah Spring Member is assumed, then a 10-m-thick slab of tuff with a density of 2.25 g/cm^3 directly underlying the repository would contain more than 25,000 metric tons of manganese oxides. This estimate is a minimum, because Mn oxides are actually concentrated along fractures rather than in the bulk rock; adequate estimates of fracture as well as bulk-rock Mn-oxide abundances will require study of large samples from exploratory mining at Yucca Mountain. Nevertheless, the waste-element retardation potential of Mn oxides at Yucca Mountain is not trivial.

VI. Fe-OXIDE VOLUME CALCULATIONS, AND THEIR LIMITATIONS AS SOLID BUFFERS FOR GROUNDWATER AT YUCCA MOUNTAIN

Using the present estimate of the volume of Fe^{2+}-bearing oxides (<0.33%) still at Yucca Mountain, we can now quantify their ability to act as solid buffers of groundwater Eh. The amount of actual Fe^{2+} oxides left in the Yucca Mountain block is less than 0.16 modal% (approximately 0.46 wt%). Of this, most of the Fe^{2+} ions in Fe-Ti oxides are isolated from groundwater because they are in densely welded tuffs of low interstitial permeability above the water table. Some of the remaining Fe^{2+}-bearing oxides already exist in reducing environments (sulfide or carbonate bearing). Therefore, the Fe-Ti oxides do not appear to buffer the groundwater below the water table at Yucca Mountain.

Many problems remain unresolved regarding the ability of Fe oxides to buffer groundwater. This is a particular problem in the unsaturated zone where available air could swamp the reducing capacity of ferrous iron in the rocks (Ogard and Kerrisk 1984). Beyond this, several other problems can be enumerated. First, will the volumes present (0.33% Fe oxides) have any long-lasting capacity for removing oxygen from the groundwater? Second, what are the kinetics of oxide mineral oxidation at low temperatures and how rapid is

the oxidation? Third, based on the kinetics of mineral oxidation and tuff alteration, how long could reduced oxide minerals buffer groundwater? Fourth, is it possible for highly oxidized unsaturated water to oxidize Fe^{2+}-bearing opaques above the static water level? Fifth, is there convection and circulation of the groundwater, or are the oxidizing, reducing, carbonaceous, and sulfide-bearing fluids stratified (convection and mixing of fluids in the groundwater would have significant implications for the ability of mineral phases to oxidize or reduce the groundwater)? And finally, what effect does the alteration of pristine glass have on groundwater and are enough reduced constituents available in glass to serve as a buffering medium? This last point is particularly important because many meters of fresh glass occur immediately below the potential repository horizon at Yucca Mountain.

VII. Eh BUFFERING POTENTIAL OF FE^{2+} IN GLASS

The thickness of vitrophyre or vitric tuff in and below the lower Topopah Spring Member varies from about 15 m to 130 m in drill cores at Yucca Mountain (Bish et al. 1983). This glass could alter, react, dehydrate, and devitrify due to increased temperatures from an overlying repository. Fe^{2+} in the glass could oxidize more rapidly during the thermal pulse following repository loading and during the containment period, or much of the Fe^{2+} in the glass could remain available for reduction during later passage of water plus waste into the glassy tuff zones during the isolation period of repository history. Whether Fe^{2+} in glass is an effective reducing agent is difficult to resolve; however, first we must demonstrate that there is indeed any Fe^{2+} to be oxidized in these glasses. Table III shows that in fact the only appreciable Fe^{2+} in bulk-rock samples from drill core USW G-4 occurs in glassy tuff below the devitrified Topopah Spring Member. The glassy tuff in the unsaturated zone below the potential repository horizon apparently provides the closest and most abundant source of ferrous iron. This topic is being addressed through glass thermal stability and oxidation studies.

VIII. CONCLUSIONS

Volume percentages have been determined for Fe^{2+}- and Mn-bearing phases at Yucca Mountain, and two conclusions can be made concerning their ability to buffer Eh conditions of the groundwater. First, the available Mn oxides are primarily Mn^{4+} minerals that have little or no potential for removing oxygen

TABLE III. FeO (wt%) IN SAMPLES FROM USW G-4[a]

Devitrified Topopah	
1089 ft	0%
1190 ft	0%
Zeolite Interval I	
1314 ft	0%
Lower Topopah Vitrophyre	
1330 ft	0.3%
Zeolite Interval II	
1438 ft	0%
1544 ft	0%
Central Prow Pass Member	
1871 ft	0%
Zeolite Interval III	
2100 ft	0%
Central Bullfrog Member	
2516 ft	0%
Zeolite Interval IV	
2716 ft	0%
2823 ft	0%

[a] Detection limit = 0.2% FeO.

from groundwater; indeed, the potential for higher-valence Mn to act as an oxidizing agent must also be investigated (Bish and Post 1984; Bartlett 1981; Murray and Dillard 1979; Hem 1978). Second, reduced Fe-Ti oxides have an upper limit of 0.33 vol%. However, much of that volume is rendered ineffective because the oxides are isolated from groundwater by a low-permeability matrix (densely welded tuff). All groundmass Fe-Ti oxides have already been oxidized to Fe^{3+}, thereby making them unsuitable as solid buffers. Therefore, only a very small percentage of oxide phenocrysts remains as buffering agents. Even at the upper limit of 0.33 vol%, any freshly exposed solid Fe-oxide buffers could react quickly, leaving the water Eh unbuffered after a short time.

Although no removal of oxygen from groundwater can be expected and oxygen removal by Fe oxides would at best occur locally and is generally insignificant, a reservoir of Fe^{2+} remains within glasses beneath the proposed repository horizon at Yucca Mountain. The potential reducing capacity of these glasses is under study, and their real reducing capacity could be modified by accelerated alteration during the thermal pulse of the repository history. Because of these uncertainties and until further data on glass

interactions are available, it is prudent to assume that the minerals and glasses have little or no capacity for reducing oxygen-rich groundwater at Yucca Mountain.

Finally, we re-emphasize the sorptive potential of Mn oxides regardless of their poor potential as reducing agents. Studies of natural trace-element migration show than Mn oxides may have an important role in sorption of heavy metals (for example, U; Zielinski 1978) that are not as effectively sorbed by zeolites as are the alkaline and alkaline-earth elements (Daniels et al. 1982). Calculations based on the data of Zielinski (1983) suggest that the small amounts of Mn oxides at Yucca Mountain may nevertheless be important retardants when summed up along the flow path. At Yucca Mountain, the selective sorption by Mn oxides could complement sorption by zeolites.

ACKNOWLEDGMENTS

Preliminary fracture data for drill cores USW G-4 and USW GU-3 were supplied by R. Spengler and R. Scott of the US Geological Survey. We greatly appreciate the use of their raw data and their continued advice and support.

We extend special thanks to D. Mann and T. Lucero who prepared high-quality polished thin sections of the ash-flow tuffs. M. Jones typed the manuscript and illustrations were prepared by J. Tubb. Initial reviews were provided by J. F. Kerrisk and H. Planner.

REFERENCES

Bartlett, R. J., "Nonmicrobial Nitrite-to-Nitrate Transformation in Soils," Soil Soc. of Amer. Jour. 45, 1054-1058 (1981).

Bish, D. L. and J. E. Post, "Thermal Behavior of Todorokite and Romanechite," Geol. Soc. Amer. Annual Mtg., Abstracts w/Program, 16, 446 (1984).

Bish, D. L., F. A. Caporuscio, J. F. Copp, B. M. Crowe, J. D. Purson, J. R. Smyth, and R. G. Warren, "Preliminary Stratigraphic and Petrologic Characterization of Core Samples from USW-G1, Yucca Mountain, Nevada," Los Alamos National Laboratory report LA-8840-MS (November 1981).

Bish, D. L., A. E. Ogard, and D. T. Vaniman, "Mineralogy-Petrology and Groundwater Geochemistry of Yucca Mountain Tuffs," in "Scientific Basis for Nuclear Waste Management VII" (Materials Research Society, Boston, 1983), 283-291.

Bower, N. W., "Simple Spectrophotometric Determination of Ferrous Iron in Twelve French Geochemical Reference Standards," Geostandards Newsletter 8, 61-62 (1984).

Byers, F. J. Jr., W. J. Carr, P. P. Orkild, W. D. Quinlivan, and K. A. Sargent, "Volcanic Suites and Related Cauldrons of Timber Mountain-Oasis Valley Caldera Complex, Southern Nevada," US Geol. Surv. Prof. Paper 919, 70 (1976).

Caporuscio, F., D. Vaniman, D. Bish, D. Broxton, B. Arney, G. Heiken, F. Byers, R. Gooley, E. Semarge, "Petrologic Studies of Drill Cores USW-G2 and UE25b-1H, Yucca Mountain, Nevada," Los Alamos National Laboratory report LA-9255-MS (July 1982).

Carroll, P. I., F. A. Caporuscio, and D. L. Bish, "Further Description of the Topopah Spring Member of the Paintbrush Tuff in Drill Holes UE-25a#1 and USW-G1 and the Lithic Rich Tuff in USW-G1, Yucca Mountain, Nevada," Los Alamos National Laboratory report LA-9000-MS (November 1981).

Christiansen, R. L., P. W. Lipman, W. J. Carr, F. M. Byers, Jr., P. P. Orkild, and K. A. Sargent, "Timber Mountain-Oasis Valley Caldera Complex of Southern Nevada," Geol. Soc. Am. Bull. 88, 943-959 (1977).

Daniels, W. R , K. Wolfsberg, R. S. Rundberg, A. E. Ogard, J. F. Kerrisk, C. J. Duffy, et al., "Summary Report on the Geochemistry of Yucca Mountain and Environs," Los Alamos National Laboratory report LA-9328-MS (December 1982).

Garrells, R. M. and Christ, C. L., Solutions, Minerals and Equilibria (Freeman, Cooper and Co., San Francisco, 1965).

Haggerty, S. W., "Oxidation of Opaque Mineral Oxides in Basalts," in Oxide Minerals, Min. Soc. Am. Short Course Notes 3, Hg-1 - Hg-100 (1976a).

Haggerty, S. W., "Opaque Mineral Oxides in Terrestrial Igneous Rocks," in Oxide Minerals, Min. Soc. Am. Short Course Notes 3, Hg-101 - Hg-300 (1976b).

Hem, J. D., "Redox Processes at Surfaces of Manganese Oxide and Their Effects on Aqueous Metal Ions," Chemical Geology 21, 199-218 (1978).

Hildreth, E. W., "The Bishop Tuff. Evidence for the Origin of Compositional Zonation in Silicic Magma Chambers," in Ash-flow tuffs, C. E. Chapin and W. Elston, eds., Geol. Soc. Am. Special Paper 180, 43-75 (1979).

Lipman, P. W., "Iron-Titanium Oxide Phenocrysts in Compositionally Zoned Ash-Flow Sheets from Southern Nevada," J. Geol. 79, 438 (1971).

Murray, J. W. and J. G. Dillard, "The Oxidation of Cobalt (II) Adsorbed on Manganese Dioxide," Geochim. et Cosmochim. Acta 43, 781-787 (1979).

Ogard, A. E. and J. F. Kerrisk, "Groundwater Chemistry Along Flow Paths Between a Proposed Repository Site and the Accessible Environment," Los Alamos National Laboratory report LA-10188-MS (November 1984).

Potter, R. M. and G. R. Rossman, "The Tetravalent Manganese Oxides: Identification, Hydration, and Structural Relationships by Infrared Spectroscopy," Am. Mineral. 64, 1199-1218 (1979a).

Potter, R. M. and G. R. Rossman, "Mineralogy of Manganese Dendrites and Coatings," Am. Mineral. 64, 1219-1226 (1979b).

Vaniman, D., D. Bish, D. Broxton, F. Byers, G. Heiken, B. Carlos, E. Semarge, F. Caporuscio, and R. Gooley, "Variations in Authigenic Mineralogy and Sorptive Zeolite Abundance at Yucca Mountain, Nevada, Based on Studies of Drill Cores USW GU-3 and G-3," Los Alamos National Laboratory report LA-9707-MS (June 1984).

Winograd, J. J. and W. Thordarson, "Hydrogeologic and Hydrochemical Framework, South-Central Great Basin, Nevada - California, with Special Reference to the Nevada Test Site," US Geol. Surv. Prof. Paper 712C (1975).

Zielinski, R. A., "Uranium Abundances and Distribution in Associated Glassy and Crystalline Rhyolites of the Western United States," Geological Soc. of Amer. Bull. 89, 409-414 (1978).

Zielinski, R. A., "Evaluation of Ash-flow Tuffs as Hosts for Radioactive Waste: Criteria based on Selective Leaching of Manganese Oxides," US Geol. Surv. Open File Report 83-480, (1983).

Zielinski, R. A., D. A. Lindsey, and J. N. Rosholt, "The Distribution and Mobility of Uranium in Glassy and Zeolitized Tuff, Keg Mountain Area, Utah, USA," Chem. Geol. 29, 139-162 (1980).

APPENDIX A

OXIDE ANALYSES

TABLE A-1. USW G-1 OXIDE MINERAL ANALYSIS (CORE)

Sample	Average (c_x)	Sample	Average	Sample	Average	Sample	Average
292	3	2486	4	4612	5.5	5212	2.5
450	6	2555	6.5	4700	6	5296	1.5
504	6	2600	6.5	4805	5.5	5312	1
619	5.5	2641	6.5	4875	5	5348	3
722	2.5	2689	6	4912	5	5412	1
757	5	2790	5.5	4998	5	5498	4
1191	4	2854	5.5	5026	5	5637	2
1240	6	2868	6.5	5093	5	5679	1
1286	4	2901	6.5	5126	5	5746	4
1291	1.5	2937	6.5	5167	3	5847	4
1392	4.5	3001	6			5947	2.5
1436	6	3116	6.5				
1561	5.5	3196	6.5				
1639	6.5	3258	6.5				
1774	6	3321	1.2				
1819	5	3371	1.3				
1854	5	3500	1.5				
1883	4	3598	2.5				
1982	2	3658	2.5				
2083	6	3706	2.5				
2166	6.5	3850	2.5				
2233	6.5	3940	7				
2247	6.5	3997	4				
2289	6	4095	6				
2290	6	4208	5.5				
2318	6	4295	5.5				
2363	6	4341	6				
2410	6.5	4400	5.5				
2436	4	4503	6				
2476	6						

TABLE A-2. USW G-2 OXIDE MINERAL ANALYSIS (CORE)

Sample	Average	Range	Sample	Average	Range
304	C_1	C_1	1634	$C_{3.0}$	$C_1 - C_5$
331	C_1	C_1	1664	$C_{5.5}$	$C_4 - C_6$
338	$C_{2.2}$	$C_1 - C_4$	1691	$C_{6.4}$	$C_6 - C_7$
358	$C_{2.0}$	$C_1 - C_4$	1745	$C_{5.3}$	$C_4 - C_7$
395	$C_{2.4}$	$C_1 - C_5$	1752	$C_{5.1}$	$C_4 - C_6$
501	$C_{3.2}$	$C_3 - C_4$	1798	$C_{5.2}$	$C_4 - C_7$
547	$C_{1.9}$	$C_1 - C_3$	1848	$C_{4.6}$	$C_3 - C_7$
561	C_3	$C_1 - C_4$	1899	$C_{5.2}$	$C_4 - C_6$
584	$C_{3.4}$	$C_1 - C_5$	1952	$C_{5.9}$	$C_4 - C_7$
627	$C_{2.4}$	$C_1 - C_5$	2001	$C_{5.8}$	$C_4 - C_7$
675	$C_{2.3}$	$C_1 - C_6$	2078	$C_{5.9}$	$C_3 - C_7$
723	$C_{1.7}$	$C_1 - C_4$	2158	$C_{6.3}$	$C_3 - C_7$
734	$C_{3.4}$	$C_1 - C_6$	2248	$C_{6.3}$	$C_5 - C_7$
762	C_2	$C_1 - C_4$	2325	$C_{6.8}$	$C_6 - C_7$
770	C_2	$C_1 - C_4$	2430	$C_{6.6}$	$C_6 - C_7$
822	C_6	$C_3 - C_7$	2528	$C_{6.6}$	$C_6 - C_7$
855	$C_{5.6}$	$C_4 - C_6$	2667	$C_{6.0}$	$C_4 - C_7$
898	C_6	$C_6 - C_7$	2744	$C_{4.6}$	$C_1 - C_7$
921	$C_{5.2}$	$C_3 - C_7$	2820	$C_{5.3}$	$C_2 - C_6$
951	$C_{3.2}$	$C_1 - C_7$	2869	$C_{5.8}$	$C_5 - C_7$
984	$C_{2.3}$	$C_1 - C_7$	2887	$C_{5.7}$	$C_4 - C_7$
1032	$C_{5.2}$	$C_1 - C_7$	2950	$C_{6.0}$	$C_6 - C_7$
1072	$C_{5.1}$	$C_2 - C_7$	2970	$C_{6.1}$	$C_5 - C_7$
1133	$C_{4.2}$	$C_1 - C_6$	3037	$C_{5.8}$	$C_4 - C_7$
1178	C_6	$C_5 - C_7$	3067	$C_{5.0}$	$C_4 - C_6$
1235	$C_{6.3}$	$C_1 - C_7$	3192	$C_{3.7}$	$C_1 - C_7$
1281	$C_{5.2}$	$C_2 - C_7$	3250[a]	$C_{5.3}$	$C_1 - C_7$
1331	$C_{5.2}$	$C_1 - C_7$	3308	$C_{6.7}$	$C_6 - C_7$
1382	$C_{3.8}$	$C_1 - C_7$	3360	$C_{3.8}$	$C_3 - C_5$
1420	$C_{5.3}$	$C_3 - C_6$	3416[a]	$C_{5.2}$	$C_1 - C_7$
1461	$C_{6.1}$	$C_4 - C_7$	3492[a]	$C_{3.0}$	$C_1 - C_7$
1585	$C_{5.1}$	$C_1 - C_7$	3541[a]	$C_{4.0}$	$C_1 - C_7$

TABLE A-2 (cont)

Sample	Average	Range	Sample	Average	Range
3671[a]	$C_{4.9}$	$C_1 - C_7$	4924	$C_{5.2}$	$C_3 - C_6$
3772[a]	$C_{6.7}$	$C_5 - C_7$	5017	$C_{1.3}$	$C_1 - C_2$
3875[a]	$C_{5.2}$	$C_4 - C_7$	5144	$C_{5.3}$	$C_5 - C_6$
3933[a]	$C_{6.9}$	$C_6 - C_7$	5206	$C_{5.6}$	$C_5 - C_7$
4005[a]	$C_{1.7}$	$C_1 - C_5$	5305[a]	$C_{5.8}$	$C_5 - C_7$
4090[a]	$C_{1.5}$	$C_1 - C_4$	5379	$C_{5.6}$	$C_5 - C_6$
4167	$C_{2.9}$	$C_1 - C_7$	5493	$C_{4.9}$	$C_4 - C_6$
4199[a]	$C_{1.3}$	$C_1 - C_2$	5596	$C_{4.3}$	$C_2 - C_6$
4209[a]	$C_{2.0}$	$C_1 - C_5$	5638	$C_{3.9}$	$C_1 - C_6$
4267	$C_{3.5}$	$C_1 - C_5$	5657	$C_{3.6}$	$C_1 - C_6$
4329	$C_{5.5}$	$C_5 - C_6$	5696	$C_{3.3}$	$C_1 - C_6$
4467	$C_{5.5}$	$C_5 - C_6$	5820	$C_{1.4}$	$C_1 - C_2$
4570	$C_{5.8}$	$C_5 - C_7$	5885	$C_{1.3}$	$C_1 - C_3$
4788	$C_{5.5}$	$C_4 - C_7$	5895	$C_{2.6}$	$C_1 - C_6$
4805	$C_{5.4}$	$C_5 - C_6$	5926	$C_{2.7}$	$C_1 - C_6$
4838	$C_{5.1}$	$C_2 - C_6$	5951	$C_{2.5}$	$C_1 - C_5$
			5992	$C_{3.6}$	$C_1 - C_5$

[a] Sulfides present.

TABLE A-3. USW GU-3 OXIDE MINERAL ANALYSIS (CORE)

Sample	Average	Range	Sample	Average	Range
31	4.6	$C_3 - C_7$	1303	3.4	$C_2 - C_6$
45	5.9	$C_2 - C_7$	1322	3.6	$C_2 - C_6$
78	5.8	$C_4 - C_7$	1394	4.4	$C_3 - C_6$
103	4.8	$C_1 - C_6$	1439	4.3	$C_2 - C_6$
245	4.5	$C_1 - C_7$	1498	3.1	$C_1 - C_7$
303	5.2	$C_4 - C_6$	1537	2.6	$C_1 - C_7$
316	5.2	$C_5 - C_6$	1571	4.8	$C_4 - C_7$
341	5.7	$C_5 - C_7$	1598	5.3	$C_1 - C_7$
356	3.4	$C_2 - C_5$	1603	6.0	C_6
376	2.2	$C_2 - C_3$	1653	6.8	$C_6 - C_7$
410	5.6	$C_4 - C_7$	1709	7.0	C_7
424	6.3	$C_4 - C_7$	1744	6.8	$C_6 - C_7$
430	3.9	$C_3 - C_5$	1874	5.2	$C_2 - C_7$
465	6.5	$C_5 - C_7$	1986	5.6	$C_5 - C_7$
482	6.3	$C_5 - C_7$	1993	5.3	$C_2 - C_7$
525	6.4	$C_6 - C_7$	2070	6.2	$C_6 - C_7$
633	4.2	$C_1 - C_7$	2138	6.0	$C_5 - C_7$
769	5.3	$C_5 - C_6$	2177	6.2	$C_6 - C_7$
954	4.0	$C_1 - C_6$	2189	5.8	$C_5 - C_7$
1130	3.7	$C_1 - C_6$	2369	4.9	$C_4 - C_6$
1175	4.0	$C_1 - C_6$	2467	4.7	$C_4 - C_6$
1195	2.7	$C_1 - C_5$	2577	4.6	$C_3 - C_6$
1227	2.2	$C_1 - C_5$			

TABLE A-4. USW G-3 OXIDE MINERAL ANALYSIS (CORE)

Sample	Average	Range	Sample	Average	Range
2615	4.9	$C_4 - C_6$	3672	6.0	C_6
2656	5.3	$C_3 - C_7$	3759[a]	3.1	$C_2 - C_4$
2695	5.7	$C_5 - C_7$	3854[a]	3.9	$C_1 - C_7$
2727	6.2	$C_5 - C_7$	4008[a]	4.3	$C_3 - C_5$
2914	6.3	$C_6 - C_7$	4240[a]	5.1	$C_4 - C_7$
3004	5.8	$C_5 - C_7$	4297[a]	5.5	$C_5 - C_6$
3045	6.2	$C_6 - C_7$	4416[a]	5.7	$C_5 - C_6$
3113	6.0	$C_5 - C_7$	4423[a]	5.5	$C_1 - C_7$
3164	6.3	$C_6 - C_7$	4568[a]	5.1	$C_2 - C_6$
3207	6.2	$C_6 - C_7$	4600	5.8	$C_1 - C_7$
3226	6.2	$C_5 - C_7$	4708[a]	5.7	$C_5 - C_7$
3310	6.2	$C_5 - C_7$	4756[a]	4.0	$C_1 - C_7$
3475	6.2	$C_5 - C_7$	4906[a]	4.0	$C_2 - C_6$
3589	6.0	$C_5 - C_7$	5014	5.3	$C_5 - C_6$

[a] Sulfides present.

TABLE A-5. USW G-4 OXIDE MINERAL ANALYSIS (CORE)

Sample	Oxidation Average	Oxidation Range
G-4-72	4.9	$C_3 - C_6$
107	5.6	$C_3 - C_7$
123	4.1	$C_2 - C_7$
147	4.3	$C_3 - C_7$
148	6.4	$C_3 - C_7$
159	3.5	$C_1 - C_6$
170	4.1	$C_2 - C_7$
220	4.3	$C_3 - C_6$
231	5.7	$C_5 - C_7$
236[a]	6.3	$C_5 - C_7$
241	7.0	C_7
383	4.4	$C_2 - C_7$
410	4.5	$C_2 - C_6$
416	5.8	$C_3 - C_7$
447	6.4	$C_6 - C_7$
514	5.6	$C_1 - C_7$
556	5.8	$C_5 - C_7$
625	5.5	$C_4 - C_7$
677	5.5	$C_5 - C_7$
692[b]	1.2	$C_1 - C_2$
746	5.5	$C_4 - C_6$
817	4.9	$C_4 - C_6$
934[c]	5.7	$C_1 - C_7$
1026	3.7	$C_1 - C_7$
1089	5.0	$C_3 - C_6$
1117	4.9	$C_3 - C_6$
1190	3.7	$C_1 - C_6$
1244	4.8	$C_2 - C_6$
1282	4.2	$C_1 - C_6$
1299	3.4	$C_1 - C_6$
1311	2.2	$C_1 - C_4$
1314	2.1	$C_1 - C_3$
1331	1.5	$C_1 - C_2$
1342[d]	2.3	$C_2 - C_4$
1381	5.9	$C_4 - C_7$
1392	4.4	$C_1 - C_7$
1419	4.2	$C_1 - C_7$
1432	4.5	$C_3 - C_7$
1432 (2)	4.1	$C_2 - C_7$
1438	5.4	$C_2 - C_7$
1470	5.1	$C_4 - C_6$
1544	5.8	$C_5 - C_7$
1544 (2)	5.5	$C_5 - C_6$
1602	6.4	$C_5 - C_7$
1685	6.1	$C_3 - C_7$
1707	6.9	$C_6 - C_7$
1702 (2)	7.0	C_7
1734	5.2	$C_4 - C_7$
1762	5.8	$C_1 - C_7$
1763	3.9	$C_2 - C_5$
1780	4.5	$C_4 - C_6$
1872	4.2	$C_3 - C_5$
1989	6.0	$C_5 - C_7$
2039	5.7	$C_5 - C_7$
2090	5.4	$C_5 - C_6$
2132	5.5	$C_4 - C_7$
2202	6.1	$C_5 - C_7$
2227	6.6	$C_6 - C_7$
2239	5.9	$C_4 - C_7$
2285	5.8	$C_5 - C_6$
2355	5.3	$C_4 - C_6$
2534	5.6	$C_5 - C_6$
2599	5.8	$C_5 - C_7$
2681	4.9	$C_4 - C_6$
2731	4.8	$C_4 - C_7$
2738	5.8	$C_5 - C_7$
2755	5.6	$C_5 - C_7$
2791	5.9	$C_5 - C_7$
2841	6.5	$C_5 - C_7$
3001	6.1	$C_5 - C_7$

[a] One pyrhottite grain.

[b] Sulfide in one magnetite grain.

[c] Mostly C_{5-7} and one C_1.

[d] Sulfide in one magnetite grain.

TABLE A-6. USW H-6 OXIDE MINERAL ANALYSIS (CORE)

Sample	Oxidation Average	Oxidation Range
1092	6.2	$C_5 - C_7$
1129	5.8	$C_4 - C_7$
1149	4.4	$C_1 - C_6$
1166	4.3	$C_2 - C_7$
1368	4.9	$C_4 - C_7$
1376	5.4	$C_4 - C_7$
1381	5.4	$C_3 - C_7$
1426	5.9	$C_5 - C_7$
1512	6.0	$C_5 - C_7$
1671	5.8	$C_3 - C_7$
1679	5.2	$C_2 - C_7$
1829	6.6	$C_6 - C_7$
2051	6.5	$C_6 - C_7$
2354	5.7	$C_4 - C_7$
2865	6.3	$C_5 - C_7$
3003	4.5	$C_3 - C_6$
3188	5.4	$C_4 - C_7$
3605	2.6	$C_1 - C_4$
3806[a]	5.5	$C_5 - C_6$

[a] Minor sulfides (pyrrhotite?) present in phenocrysts of USW H-6-3806.

TABLE A-7. UE-25p#1 OXIDE MINERAL ANALYSIS (CUTTINGS, SIDEWALL SAMPLES AND CORE)

Sample	Oxidation Average	Oxidation Range	Comments
120	5.4	$C_1 - C_7$	
210	4.8	$C_1 - C_7$	
270	1.5	$C_1 - C_2$	4 Fe-Ti-oxide phenocrysts
290	1.1	$C_1 - C_2$	4 Fe-Ti-oxide phenocrysts
420	6.6	$C_6 - C_7$	
580	4.9	$C_4 - C_5$	7 Fe-Ti-oxide phenocrysts
620	4.2	$C_3 - C_6$	5 Fe-Ti-oxide phenocrysts
910	4.9	$C_3 - C_6$	
1050	4.0	$C_3 - C_5$	5 Fe-Ti-oxide phenocrysts
1150	5.4	$C_5 - C_6$	8 Fe-Ti-oxide phenocrysts
1250	5.5	$C_5 - C_6$	4 Fe-Ti-oxide phenocrysts
1270	5.3	$C_5 - C_6$	4 Fe-Ti-oxide phenocrysts
1290[a]	6.0	C_6	4 Fe-Ti-oxide phenocrysts
1350	5.0	C_5	4 Fe-Ti-oxide phenocrysts
1400[a]	7.0	C_7	
1420[a]	6.0	$C_1 - C_7$	
1470[a]	5.4	$C_4 - C_7$	
1598	6.3	$C_4 - C_7$	
1650	6.7	$C_6 - C_7$	7 Fe-Ti oxide phenocrysts
1700	4.7	$C_4 - C_6$	
1740	5.6	$C_5 - C_7$	
1800	5.9	$C_5 - C_7$	
1840	5.5	$C_5 - C_6$	
1930	5.0	$C_4 - C_6$	
2000	5.5	$C_5 - C_6$	
2220	5.5	$C_5 - C_7$	
2250	5.8	$C_5 - C_7$	
2290	5.5	$C_5 - C_7$	
2380	5.4	$C_5 - C_6$	7 Fe-Ti oxide phenocrysts
2520	5.8	$C_5 - C_6$	
2580	5.6	$C_4 - C_7$	

TABLE A-7 (cont)

Sample	Oxidation Average	Oxidation Range	Comments
2640	5.7	$C_5 - C_7$	
2660	6.3	$C_5 - C_7$	
2760	6.1	$C_1 - C_7$	
2900	5.0	$C_4 - C_6$	
2950	5.5	$C_4 - C_7$	
3170	5.3	$C_5 - C_6$	
3240	5.0	$C_5 - C_7$	
3330	5.3	$C_4 - C_6$	
3453.3	5.1	$C_5 - C_6$	
3560	5.0	$C_4 - C_6$	
3570	4.4	$C_4 - C_5$	
3600	5.7	$C_5 - C_6$	
3640	5.5	$C_4 - C_6$	
3660	4.5	$C_4 - C_5$	
3670	4.5	$C_4 - C_5$	
3730	2.3	$C_1 - C_3$	
3913[b]	6.0	$C_5 - C_7$	
3916.8[b]	5.7	$C_5 - C_7$	
3928[b]			Sulfides only
3970	5.7	$C_5 - C_6$	
3990	6.2	$C_5 - C_7$	

[a] Sidewall samples.
[b] Core.

TABLE A-8. UE-25a#1 OXIDE MINERAL ANALYSIS (CORE)

Sample	Average	Range
YM38	C_5	C_4 - C_6
YM45	C_4	C_3 - C_5
YM48	C_6	C_5 - C_7
YM49	C5	C_4 - C_6
YM54	C_5	C_4 - C_7

TABLE A-9. UE-25b#1 OXIDE MINERAL ANALYSIS (CORE)

Sample	Average	Range	Sample No.	Average	Range
2402	$C_{5.6}$	C_5 - C_6	3225	$C_{5.8}$	C_5 - C_6
2525	$C_{6.4}$	C_6 - C_7	3[illegible]	$C_{6.0}$	C_6
2596	$C_{6.5}$	C_6 - C_7	3322	$C_{6.2}$	C_6 - C_7
2737	$C_{6.7}$	C_6 - C_7	3393[a]	$C_{1.5}$	C_1 - C_2
2832	$C_{6.6}$	C_5 - C_7	3469[a]	-	
2855	$C_{6.1}$	C_5 - C_7	3506[a]	-	
2879	$C_{5.5}$	C_4 - C_7	3771A[a]	C_4	1 grain
2919	$C_{6.4}$	C_6 - C_7	3571B[a]	C_1	1 grain
2953	$C_{5.8}$	C_5 - C_6	3660[a]	C_1	C_1
3050	$C_{6.0}$	C_5 - C_7	3767[a]	$C_{1.2}$	C_1 - C_2
3095	$C_{5.3}$	C_5 - C_6	3835[a]	$C_{1.2}$	C_1 - C_2
3018	$C_{6.1}$	C_5 - C_7	3902[a]	-	
3163	$C_{5.7}$	C_5 - C_7	3910[a]	C_1	1 grain
3185	$C_{5.7}$	C_4 - C_7	3956[a]	C_2	C_1 - C_3
3196	$C_{6.0}$	C_5 - C_7	3988[a]	$C_{1.7}$	C_1 - C_3

[a] Sulfides present.

☆ U.S. GOVERNMENT PRINTING OFFICE 1985—576-034/20055